BJR

Received: 11 January 2015 | Revised: 2 March 2015 | Accepted: 3 March 2015

doi: 10.1259/bjr.20150034

Cite this article as:
Liney GP, Holloway L, Al Harthi TM, Sidhom M, Moses D, Juresic E, et al. Quantitative evaluation of diffusion-weighted imaging techniques for the purposes of radiotherapy planning in the prostate. Br J Radiol 2015;88:20150034.

FULL PAPER

Quantitative evaluation of diffusion-weighted imaging techniques for the purposes of radiotherapy planning in the prostate

[1,2,3]G P LINEY, PhD, [1,2,3,4]L HOLLOWAY, PhD, [4]T M AL HARTHI, MSc, [1]M SIDHOM, MB BS, [1]D MOSES, MB BS, [1]E JURESIC, MSc, [1]R RAI, MSc and [5]D J MANTON, PhD

[1]Liverpool Cancer Therapy Centre and Ingham Institute, Liverpool Hospital, Sydney, NSW, Australia
[2]South Western Sydney Clinical School, University of New South Wales, Sydney, NSW, Australia
[3]Centre for Medical Radiation Physics, University of Wollongong, Wollongong, NSW, Australia
[4]Institute of Medical Physics, School of Physics, University of Sydney, Sydney, NSW, Australia
[5]Radiation Physics, Hull and East Yorkshire Hospitals NHS Trust, Castle Hill Hospital, Hull, UK

Address correspondence to: Associate Professor Gary P Liney
E-mail: *Gary.Liney@sswahs.nsw.gov.au*

Objective: Diffusion-weighted imaging (DWI) is an important technique for the localization of prostate cancer, and its response assessment during treatment with radiotherapy (RT). However, it has known limitations in terms of distortions and artefacts using standard acquisition techniques. This study evaluates two alternative methods that offer the promise of improved image quality and the potential for more reliable and consistent diffusion data.

Methods: Three DWI techniques were investigated; single-shot echoplanar imaging (EPI), EPI combined with reduced volume excitation (ZOOMit; Siemens Healthcare, Erlangen, Germany) and read-out segmentation with navigator-echo correction (RESOLVE; Siemens Healthcare). Daily measurements of apparent diffusion coefficient (ADC) value were made in a quality assurance phantom to assess the repeatability of each sequence. In order to evaluate the geometric integrity of these sequences, ten normal volunteers were scanned, and the prostate was contoured to compare its similarity with T_2 weighted images.

Results: Phantom ADC values were significantly higher using the standard EPI sequence than those of the other two sequences. Differences were also observed between sequences in terms of repeatability, with RESOLVE and EPI performing better than ZOOMit. Overall, the RESOLVE sequence provided the best agreement for the *in vivo* data with smaller differences in volume and higher contour similarity than T_2 weighted imaging.

Conclusion: Important differences have been observed between each of the three techniques investigated with RESOLVE performing the best overall. We have adopted this sequence for routine RT simulation of prostate patients at Liverpool Cancer Therapy Centre.

Advances in knowledge: This work will be of interest to the increasing number of centres wanting to incorporate quantitative DWI in a clinical setting.

MRI has a number of advantages for radiotherapy (RT) planning of prostate cancer, including its excellent soft-tissue contrast and the ability to acquire functional information. At present, MRI is primarily used in RT to improve delineation of the whole gland and organs at risk, which has been shown to be superior to that obtained from using CT.[1] With developments of highly conformal RT, functional MRI techniques, which demonstrate macroscopic tumour nodules, are of significant interest and could potentially be used to target a boost in radiation rather than escalate dose to the whole gland.[2] One such technique of particular relevance is diffusion-weighted imaging (DWI), which utilizes strong bipolar gradients to sensitize the sequence to microscopic molecular diffusion.[3] The diffusion weighting is characterized by the strength and timing of these gradients and described collectively by a coefficient referred to as the "*b*-value" of the image. Images with at least two different *b*-values, usually a zero or low value and a second higher value, can be acquired to measure the apparent diffusion coefficient (ADC). Diffusion that is restricted owing to the cellular environment demonstrates high signal on the *b*-value images and low ADC values compared with free diffusion. These ADC values have been correlated with histological measurements of cell density in prostate tumours with low ADC reflecting a higher degree of cellularity.[4] DWI has been shown to be useful in prostate tumour detection and localization with a high degree of sensitivity when either used on its own or

in combination with other imaging parameters.[5,6] In addition, some groups have begun to acquire DWI during RT and have shown increases in tumour ADC values reflecting a response in treatment that could be useful in monitoring and prospectively adapting RT delivery.[7]

However, the vast majority of DWI studies to date have been implemented using the standard echoplanar imaging (EPI) pulse sequence, which is prone to image artefacts, including Nyquist ghosting owing to phase errors and anatomical distortions owing to susceptibility variations.[8] These artefacts are worse at higher field strengths and are the likely cause of poor reproducibility seen at 3.0 T.[9] Image quality is improved somewhat by acquiring EPI in multiple segments rather than as a single-shot acquisition. This segmentation is generally in the phase-encoding direction and extends the overall scan time. Other previous solutions have been to combine DWI with other image acquisitions (*e.g.* HASTE) or with radial k-space sampling strategies (*e.g.* BLADE, PROPELLER).[10,11]

In the past couple of years, two new approaches to the problem of diffusion-weighted image quality have been proposed, which have recently been implemented as commercially available sequences. The first takes advantage of parallel radiofrequency (RF) transmission technology, which was principally developed to remedy dielectric effects at high field. The use of separate transmitter waveforms can be exploited to obtain a shaped or focused excitation of a reduced volume.[12] In doing so, the image can be limited to the tissue of interest, and when combined with DWI, tissues contributing to artefacts can be omitted from signal acquisition. This method has been recently reported as improving prostate DWI quality in terms of reduced distortion and clarity of the prostatic capsule.[13] A second technique utilizes segmentation but in the other (read-out) encoding direction, which can be used on its own[14] or in combination with a navigator echo for the correction of motion-induced or other sources of phase errors.[15] This type of sequence has been shown to provide higher diagnostic accuracy in breast lesions at 3.0 T.[16]

If diffusion data are to be included in RT planning process, then these improvements in DWI must translate beyond simply the perceived increase in image quality. It is clear that ADC values must be shown to be reproducible and that anatomy must be geometrically accurate if RT plans are to be based on this information. The purpose of this work was to evaluate the efficacy of two new DWI techniques, which we acquired on our newly installed scanner, for their potential to be used in RT planning of the prostate. The first technique (ZOOMit; Siemens Healthcare, Erlangen, Germany) is the focused excitation method, which currently can only be used with two pulse sequences one of which is EPI. The second sequence (RESOLVE; Siemens Healthcare) is based on the read-out segmentation with a navigator echo correction approach. In this study, these techniques were compared against the current gold-standard method of acquiring DWI data, namely single-shot EPI, in terms of both ADC repeatability *in vitro* and anatomical integrity of the prostate *in vivo*. Results suggest important quantitative differences that to our knowledge have not been presented before. Although primarily aimed with RT planning in mind, this study will be of interest to both the radiation oncology and radiology communities.

METHODS AND MATERIALS

All imaging was performed on a dedicated wide-bore 3.0-T system (MAGNETOM® Skyra, Siemens Healthcare, Erlangen, Germany) equipped with XQ gradients, which is used at Liverpool Cancer Therapy Centre for the planning ("MR-Simulation") of RT in patients. A doped [nickel(II) sulfate] water phantom was imaged in a 20-channel RF head coil on a daily basis over a period of 1 month in order to assess both the short- (daily) and long-term (weekly) repeatability of each DWI sequence described below. The temperature of the scanner room was controlled at a constant temperature, and the temperature within the bore was recorded throughout the scanning sessions using the system thermometer. ADC maps were generated using a monoexponential fit of the DWI data using the manufacturer's software on the scanner console. Regions of interest at the centre slice and covering approximately 80% of the signal-producing area were used to provide the ADC value.

Statistical analysis was carried out using Microsoft Excel® (Microsoft, Redmond, WA). Systematic differences in mean ADC values between sequences were assessed using unpaired, Student's *t*-tests. Repeatability was quantified using the methodology of Bland and Altman.[17] The long-term coefficient of repeatability was calculated as 2.77 times the standard deviation of ADC values repeated on different days. The short-term (same-day) coefficient of repeatability was calculated as 2.77 times the (within-day's) standard deviation of the individual ADC values repeated on different days, after subtraction of the respective daily means in order to remove between-day variations [first ADC (Day 1) − mean ADC (Day 1), second ADC (Day 1) − mean ADC (Day 1), first ADC (Day 2) − mean ADC (Day 2) etc.]. Differences in repeatability between sequences were assessed using the *F*-test for equality of variances acting on raw ADC values for long-term data and daily mean-subtracted ADC values for short-term data.

In order to quantify anatomical distortion *in vivo*, a total of ten normal subjects (aged between 19 and 55 years) were examined using the 32-channel RF coil in the patient table in combination with the 18-channel flexible torso RF coil strapped to the abdomen. Local ethics permission was granted by South Western Sydney local health district to carry out these investigations. Imaging included the three diffusion techniques described below plus an axial T_2 weighted turbo spin echo acquisition [echo time (TE)/repetition time (TR) = 87/5330 ms] with a slice thickness of 2.00- and 0.75-mm in-plane resolution and a pixel bandwidth of 440 Hz per pixel, which was taken as the gold standard data set. For the DWI scans, three sequences were tested, which were single-shot EPI, RESOLVE and EPI with shaped (ZOOMit) excitation. In each case, imaging parameters were kept as similar as possible, allowing for the inherent differences between sequences, and a total of 20 slices were acquired. Diffusion parameters included three *b*-values (50, 400 and 800 mm s^{-2}), which were acquired with an increasing number of signal averages to account for reduction in signal-to-noise ratio observed at the longest *b*-value.[18] Specifically, these values were 4, 7 and 10 (EPI); 1, 1 and 3 (RESOLVE); and 2, 4 and 10 (ZOOMit). Other imaging parameters included TE/TR = 54–88/3900–4300 ms with a field of view (FOV) of 21 cm and in-plane resolution of 1.7 mm with slice thickness of 4 mm. The ZOOMit

Table 1. Mean apparent diffusion coefficient (ADC) (± standard deviation) and coefficient of repeatability values obtained in a doped water phantom for each of the diffusion-weighted imaging sequences investigated

Measurement	Echoplanar imaging	RESOLVE	ZOOMit
ADC	1.910 ± 0.026	1.875 ± 0.025	1.891 ± 0.039
Short-term repeatability	0.0155 (0.80%)	0.0125 (0.66%)	0.0597 (3.11%)
Long-term repeatability	0.0620 (3.26%)	0.0667 (3.57%)	0.1183 (6.27%)

All units are $\times 10^{-3}$ mm^2 s^{-1}; percentage values are also given with respect to the corresponding mean values for data used in repeatability calculations.

sequence was acquired with a 60% reduction in the FOV in the phase direction. The RESOLVE and EPI sequences were also used in conjunction with the parallel imaging technique GRAPPA[19] set at a factor of 2. Acquisition times for each sequence were 4 min 27 s (EPI), 7 min 3 s (RESOLVE) and 3 min 32 s (ZOOMit).

The $b = 50$ s mm^{-2} images were registered to the T_2 weighted images using an automated (rigid-body) registration process on the scanner workstation to provide a subjective comparison of the geometrical accuracy. These same scans were then exported to a treatment planning workstation (Pinnacle; Philips Medical Systems) for subsequent analysis with the DWI sequences being de-identified. The whole prostate gland contour was delineated on all slices for the T_2 weighted series and each DWI sequence by both a trained radiologist and oncologist independently of each other. All contours were then transferred onto a personal computer for subsequent calculation of the total prostate gland volume and Dice's similarity coefficient (DSC)[20] using in-house written code.

Finally, the DWI sequence, which was deemed to have performed best overall in terms of geometry and ADC, was additionally investigated further in the same volunteer by acquiring DWI scans on three separate examinations. This involved the subject being removed and repositioned on the bed prior to each scan session, which was undertaken within a period of 60 min. Regions of interest within the right peripheral zone were drawn based on the $b = 50$ s mm^{-2} images, and these were copied directly onto the ADC maps to obtain the diffusion values for each scan session.

RESULTS

Table 1 gives results from the phantom measurements, which were all recorded within a temperature range of 19.5 ± 0.1 °C. Both ADC and coefficient of repeatability values are shown, with the latter also showing the percentage with respect to the mean. ADC values ranged from 1.82 to 1.97 mm^2 s^{-1}, which are in-line with what has previously been reported for water at the temperature of our scan room.[21] Mean ADC values were significantly higher with EPI than with the other two sequences ($p < 0.001$). In terms of repeatability, both EPI and RESOLVE were shown to be significantly more repeatable than ZOOMit ($p < 0.05$) over the short-term data. Longer-term repeatability was worse than the short-term values in all cases as was expected. Differences were again observed between the three sequences with EPI and RESOLVE, providing more repeatable long-term data, although this was not statistically significant ($p < 0.15$).

Figure 1 shows an example of the prostate DWI ($b = 50$ s mm^{-2}) images acquired with each of the three sequences fused to the corresponding T_2 weighted image at the same slice location. The EPI sequence shows a small discrepancy at the edge of the right peripheral zone indicating geometric distortion. In comparison, both the RESOLVE and ZOOMit sequences demonstrate a better registration result in the prostate. When the results of the contouring study were analysed quantitatively (Table 2), it was found that RESOLVE produced the best agreement with the T_2 weighted data, as evidenced by both the smallest mean volume difference (3.77 cm^3) and the largest mean DSC score (0.74). This result was consistent for both observers. On average, the smallest DSC values were obtained with ZOOMit (mean of 0.66). The largest volume difference was observed with the EPI sequence with a 5.99-cm^3 or 21% difference. Multiple examinations of the same volunteer were undertaken using the RESOLVE sequence; the mean ADC value within the same normal peripheral zone region was found to be 1.353, 1.397 and 1.356 mm^2 s^{-1}, respectively.

CONCLUSIONS

DWI offers a lot of promise for RT planning of prostate cancer, although incorporation of these data into the treatment planning

Figure 1. (Left to right) Example diffusion-weighted images acquired with $b = 50$ mm s^{-2} for echoplanar imaging, RESOLVE and ZOOMit sequences (in orange) overlaid onto a corresponding T_2 weighted image having been the first registered. For colour images please see online version.

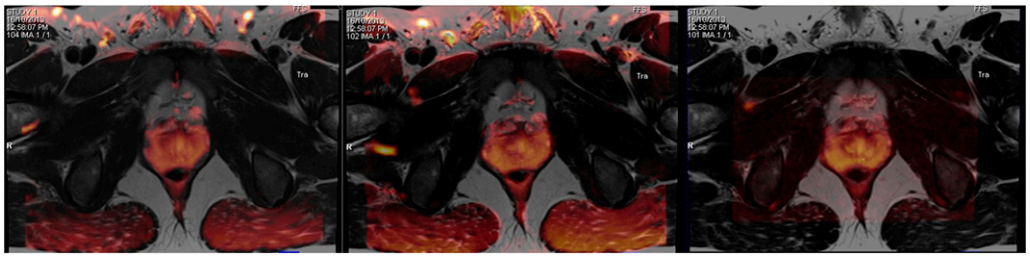

Table 2. Results from the contouring study from the two observers

Sequence	Observer 1		Observer 2	
	Volume difference (cm^3)	DSC	Volume difference (cm^3)	DSC
Echoplanar imaging	4.11	0.695	5.99	0.706
RESOLVE	3.56	0.737	3.77	0.739
ZOOMit	4.25	0.664	5.13	0.679

DSC, Dice's similarity coefficient.
Mean total volume differences between the prostate volumes determined on the T_2 weighted images and DWI sequences are given as well as the resulting DSCs obtained from the contour comparison.

process is still in its infancy, and improvements in image quality are necessary if this is to become routinely implemented. Geometrically, accurate data sets are vital if treatment plans are to be designed to target lesions within the gland. Reliable ADC values are required if these are to be used as subsequent thresholds for monitoring and adapting to response or failure of treatment. Some early studies by others have demonstrated improvements in DWI using some of the newer acquisition techniques, including the two described here, albeit these have been investigated only qualitatively and in isolation. We believe this is the first time differences between these three DWI sequences have been quantified alongside each other in the manner reported here.

We have shown important quantitative differences between three commercially available DWI sequences at 3.0 T. We have carried this out by taking measurements in a uniform phantom as well as in a cohort of prostate subjects and, in doing so, demonstrated that one of these sequences may be preferred in the context of RT planning. This was evaluated by first looking at the ADC value in water over a number of occasions at a controlled temperature. Interestingly, the standard EPI sequence produced significantly higher values of ADC than did the other sequences. The repeatability was shown to be poorer using ZOOMit than the other two sequences. When including a comparison of the *in vivo* data, RESOLVE appears to be the most robust and reliable of the methods examined. This sequence produced the highest DSC values and the smallest difference in prostate volume for both observers. Without a non-imaging gold standard, the DSC is a commonly used spatial overlap index and reproducibility validation metric. Values range from 0, indicating no overlap, to 1, indicating a complete overlap. High values are desirable but scores >0.7 have been considered useful and have been used in segmentation studies as evidence of a successful outcome.[22,23] In practice, inclusion of ADC information into the MR simulation workflow would involve registering the DWI data set to the anatomical images from the same examination, and the sequence with the highest DSC value would be clearly preferable. This combined data set could then be contoured on the treatment planning system.

The three repeat DWI examinations using the RESOLVE technique produced ADC values in the same normal tissue region that were within 3.25% of each other. Although a limitation here is that this was only performed in a single subject and therefore no statistical meaning could be drawn, it was nevertheless a further attempt to assess *in vivo* consistency with this sequence. These measurements will include confounding factors such as set-up and partial volume but gives an indication as to the underlying variation that may be expected in clinical cases. To put this into context, Park et al[7] reported increases in mean tumour ADC in 13 patients from a pre-treatment value of 0.86–1.26 post treatment, whereas changes in between weeks 1 and 3 of treatment were shown to be as little as 10%. This underlines the importance of using a consistent and reliable sequence, particularly when serial data sets are being interpreted to assess response.

It is important to remember that both these new techniques still use EPI as the underlying sequence module but offer potential improvements in terms of the way this sequence is implemented. Focused excitation is an inherently quicker method and could be used to provide higher spatial resolution, but it did not provide the best quantitative results in this study. Segmentation in the read-out direction means phase encoding is carried out in one continuous trajectory, which is an advantage over phase segmentation. The additional use of a navigator echo enables inconsistent data to be corrected or even discarded albeit at the cost of an increased scan time. In this study, the RESOLVE sequence was double the scan time of the shortest DWI scan (ZOOMit). This is a consideration, as prolonged examination times could have a deleterious effect on prostate movement secondary to bladder filling or rectum filling, for example. Nevertheless, we have shown that this technique provides the most robust and reliable data set and would seem to be the preference for RT planning studies.

The observed advantages of this sequence are likely to be of further importance in prostate cases with challenging susceptibility environments such as rectal gas and seed implants. Although we were chiefly interested in its potential for RT, these findings are important to radiology generally, and this technique may have other advantages, for example, to help prostate biopsy or obviate the need for rectum preparation. There may also be specific advantages at the apex of the gland, although this was not separately examined in this study and requires further investigation. In conclusion, we have adopted RESOLVE as our DWI sequence of choice at our clinic and are routinely acquiring these data sets not only in prostate but also cervix and rectum studies.

FUNDING

We would like to acknowledge the financial support of the Ingham Institute for Applied Medical Research.

REFERENCES

1. Villiers GM, Van Vaeranbergh K, Vakaet L, Bral S, Claus F, De Neve WJ, et al. Inter observer delineation variation using CT versus combined CT + MRI in intensity modulated radiotherapy for prostate cancer. *Strahlenther Onkol* 2005; **181**: 424–30.
2. Bauman G, Haider M, Van der Heide UA, Ménard C. Boosting imaging defined dominant prostatic tumours: a systematic review. *Radiother Oncol* 2013; **107**: 274–81. doi: 10.1016/j.radonc.2013.04.027
3. Stejskal EO, Tanner JE. Spin diffusion measurements: spin echoes in the presence of a time-dependent field gradient. *J Chem Phys* 1965; **42**: 288–92.
4. Gibbs P, Liney GP, Pickles MD, Zelhof B, Rodrigues G, Turnbull LW. Correlation of ADC and T2 measurements with cell density in prostate cancer at 3.0 Tesla. *Invest Radiol* 2009; **44**: 572–6. doi: 10.1097/RLI.0b013e3181b4c10e
5. Isebaert S, Van den Bergh L, Haustermans K, Joniau S, Lerut E, De Wever L, et al. Multi parametric MRI for prostate cancer localization in correlation to whole-mount histopathology. *J Magn Reson Imaging* 2013; **37**: 1392–401. doi: 10.1002/jmri.23938
6. Jin G, Su DK, Luo NB, Liu LD, Zhu X, Huang XY. Meta-analysis of diffusion-weighted magnetic resonance imaging in detecting prostate cancer. *J Comput Assist Tomogr* 2013; **37**: 195–202. doi: 10.1097/RCT.0b013e3182801ae1
7. Park SY, Kim CK, Park BK, Park W, Park HC, Han DH, et al. Early changes in apparent diffusion coefficient from diffusion-weighted MR imaging during radiotherapy for prostate cancer. *Int J Radiat Oncol Biol Phys* 2012; **83**: 749–55. doi: 10.1016/j.ijrobp.2011.06.2009
8. Mansfield P, Pykett IL. Biological and medical imaging by NMR. *J Magn Reson* 1978; **29**: 355–73.
9. Gibbs P, Pickles MD, Turnbull LW. Repeatability of echo-planar-based diffusion measurements of the human prostate at 3T. *Magn Reson Imaging* 2007; **25**: 1423–9.
10. Babourina-Brooks B, Cowin GJ, Wang D. Diffusion-weighted imaging in the prostate: an apparent diffusion, coefficient comparison of half-Fourier acquisition single-shot turbo spin-echo and echo planar imaging. *Magn Reson Imaging* 2012; **30**: 189–94. doi: 10.1016/j.mri.2011.09.024
11. Schwartz KM, Lane JI, Bolster BD Jr, Neff BA. The utility of diffusion-weighted imaging for cholesteatoma evaluation. *AJNR Am J Neuroradiol* 2011; **32**: 430–6. doi: 10.3174/ajnr.A2129
12. Rieseberg S, Frahm J, Finsterbusch J. Two-dimensional spatially-selective RF excitation pulses in echo-planar imaging. *Magn Reson Med* 2002; **47**: 1186–93.
13. Rosenkrantz AB, Geppert C, Pfeuffer J, Mossa DJ, Chandarana H. Zoomed EPI using parallel transmission: impact on image quality of diffusion-weighted imaging of the prostate at 3T. In: Proceedings of ISMRM; New York, NY. 2013. pp. 3390.
14. Yeom KW, Holdsworth SJ, Van AT, Iv M, Skare S, Lober RM, et al. Comparison of read-out segmented echo-planar imaging (EPI) and single-shot in clinical application of diffusion-weighted imaging of the pediatric brain. *AJR Am J Roentgenol* 2013; **200**: 437–43. doi: 10.2214/AJR.12.9854
15. Porter DA, Heidemann RM. High resolution diffusion-weighted imaging using read-out segmented echo-planar imaging, parallel imaging and a two-dimensional navigator-based reacquisition. *Magn Reson Med* 2009; **62**: 468–75. doi: 10.1002/mrm.22024
16. Bogner W, Pinker-Domenig K, Bickel H, Chmelik M, Weber M, Helbich TH, et al. Read-out segmented echo-planar imaging improves the diagnostic performance of diffusion-weighted MR breast examinations at 3.0 T, *Radiology* 2012; **263**: 64–76. doi: 10.1148/radiol.12111494
17. Bland JM, Altman DG. Measuring agreement in method comparison studies. *Stat Methods Med Res* 1999; **8**: 135–60.
18. Bito Y, Hirata S, Yamamoto E. Optimal gradient factors for ADC measurements. In: Proceedings of the 3rd Annual Meeting of the International Society for Magnetic Resonance in Medicine; Nice, France. 1995. pp. 913.
19. Griswold MA, Jakob PM, Heidemann RM, Nittka M, Jellus V, Wang J, et al. Generalized autocalibrating partially parallel acquisitions (GRAPPA). *Magn Reson Med* 2002; **47**: 1202–10.
20. Dice LR. Measures of the amount of ecologic association between species. *Ecology* 1945; **26**: 297–302.
21. Tofts PS, Lloyd D, Clark CA, Barker GJ, Parker GJ, McConville P, et al. Test liquids for quantitative MRI measurements of self-diffusion coefficient *in vivo*. *Magn Reson Med* 2000; **43**: 368–74.
22. Xue H, Srinivasan L, Jiang S, Rutherford M, Edwards AD, Rueckert D, et al. Automatic segmentation and reconstruction of the cortex from neonatal MRI. *Neuroimage* 2007; **38**: 461–77.
23. Zijdenbos AP, Dawant BM, Margolin RA, Palmer AC. Morphometric analysis of white matter lesions in MR images: method and validation. *IEEE Trans Med Imaging* 1994; **13**: 716–24.